Solid-State NMR Characterization of the Surfactant–Silica Interface in Templated Silicas: Acidic versus Basic Conditions

Niki Baccile, Guillaume Laurent, Christian Bonhomme, Plinio Innocenzi, Florence Babonneau

Solid State NMR characterization of the surfactant/silica interface in templated silicas: acidic versus basic conditions.

*Niki Baccile[a], Guillaume Laurent[a], Christian Bonhomme[a], Plinio Innocenzi[b] and Florence Babonneau[a]**

[a] Laboratoire de Chimie de la Matière Condensée de Paris, Université Pierre et Marie Curie-Paris6; CNRS, 4 place Jussieu, 75252 Paris Cedex 05, France

[b]Dipartimento di Architettura e Pianificazione (Laboratorio di Scienza dei Materiali e Nanotecnologie), Università di Sassari and INSTM, Palazzo Pou Salit, Piazza Duomo 6, 07041 Alghero (Sassari), Italy

* Corresponding author : fb@ccr.jussieu.fr

RECEIVED DATE (to be automatically inserted after your manuscript is accepted if required according to the journal that you are submitting your paper to)

KEYWORDS: Mesoporous materials, Silica, Solid state NMR, HETCOR, CTAB, MCM-41, SBA-3, FT-IR spectroscopy

ABSTRACT. Combination of one-dimensional and two-dimensional solid state magic angle spinning nuclear magnetic resonance (MAS NMR) experiments has been used to investigate the hybrid organic-inorganic interfaces in surfactant templated silicas. Samples prepared with cetyltrimethylammonium

bromide (CTAB) under acidic (HCl) and basic (NaOH) conditions have been compared. The use of sequences based on the ^{29}Si-^{1}H heteronuclear dipolar interactions allows us to selectively filter the NMR response of the protons close to the Si surface sites showing directly the clear difference between the two systems. The basic sample is characterised by a small amount of Si-OH groups, and a short distance between the $Si\text{-}O^-$ surface groups and the surfactant polar head group, while the acidic sample exhibits a silanol-rich surface with a longer distance between the Si surface sites and the polar head groups. The nature of the interface induces consequent differences in the structure of the adsorbed water layers present at the interface, and this has been revealed by near infrared experiments, as well as ^{1}H MAS NMR spectra recorded on dehydrated and partially re-hydrated samples. One objective of this work was also to show that the use of standard solid state NMR conditions (magnetic field of 7 T and magic angle spinning frequency less than 15 kHz) can be largely sufficient to get extremely valuable information regarding the silica/surfactant interfaces.

1. Introduction

In the past fifteen years a large number of studies has been focused on long-range ordered mesoporous materials obtained in solution through the self-assembly of a variety of amphiphilic templating agents with a growing inorganic phase.[1] Their structural characteristics (high surface area; tunable geometry of the porous network; narrow pore size distribution)[2] combined with the possibility to process them in various shapes[3] (calibrated spherical powders[4], thin films[5], membranes, monoliths[6]) make them extremely attractive for a wide range of applications in the fields of catalysis[7,8,9], chromatography[10], drug release[11], sensors[12], electronics[13] or environment.[14,15] Moreover, the large versatility associated with a relative simplicity of the synthetic protocols has certainly contributed to the immediate interest of the community of chemists for this class of materials. Just by playing with experimental parameters such as the inorganic precursor, the type of surfactant, the pH of the solution, the temperature, the nature of co-solvents, mesoporous materials with a large range of nanostructures can be synthesized.

Despite this abundant literature, relatively few studies have been focused on a detailed

characterization of the interactions that develop between the structuring agents and the inorganic species. These interactions are of key importance to drive the self-assembly process, and to lead to the formation of a given silica/surfactant mesophase. Several research groups have focused on the understanding of the formation mechanism and reviews are dedicated to this topics, not only in the case of powders obtained through precipitation[16,17], but also in the case of thin films prepared via evaporation-induced self-assembly.[18] Less works have been centred on the description of the inorganic/organic interfaces in the final materials. Nevertheless, the way the templating molecules interact with the inorganic walls strongly influence important structural features. Upon removal of the surfactant species, an ordered mesoporous inorganic solid can result, whose typically amorphous framework structure is a replica of the hydrophilic mesophase regions and whose pores are vestiges of the hydrophobic components. Consequently, if hydrophilic parts of the structuring agents are embedded in the inorganic framework during the condensation step, then microporosity can be created. This has been already illustrated with the synthesis of mesoporous SBA-15 silica that uses the P123 poly(ethylene oxide)-poly(propylene oxide)- poly(ethylene oxide) block copolymer (EO_{20}-PO_{70}-EO_{20}). Galarneau *et al.* have shown that for a synthesis temperature below 95°C, the SBA-15 sample presents microporosity. This was explained by the presence of polyethylene oxide PEO chains at the surface of the micellar aggregates that are lately embedded in the silica network, leading to the formation of micropores after removal of the template.[19,20]

A key technique to investigate the organic/inorganic interfaces is high-resolution solid state NMR. The cross-polarisation (CP) sequence, based on through-space heteronuclear dipolar interactions, allows probing spatial proximities between the protons of the templating molecules and the selected nuclei present at the pore surface. Chmelka *et al.* very nicely illustrated this by using two-dimensional (2D) $^{29}Si\{^{1}H\}$ as well as $^{27}Al\{^{1}H\}$ heteronuclear correlation (HETCOR) experiments to investigate the distribution of PEO and polypropylene oxide PPO copolymer blocks within the silica matrix[21], the aluminum incorporation in MCM-41 mesophases[6,22] as well as the molecular proximities between the

structure-directing surfactant molecules and the crystal-like silicate sheets in layered silicate surfactant mesophases.[23] One can also use high resolution ^{1}H MAS NMR and the associated Double Quantum (DQ) NMR spectroscopy to look for proximities between the Si-OH surface sites and the template molecules. Due to the high sensitivity of such NMR experiments, Alam *et al.* applied them to silicate thin films templated with the non ionic surfactant Brij® 56, a polyoxyethylene(10) cetyl ether, and demonstrated a close spatial contact between the surfactant and the silica framework, through Si-O-$\underline{H}$….O-C$\underline{H}_2$ proximities.[24] Additionally, some studies have been focused on the behaviour of the surfactant molecules using ^{13}C NMR experiments.[25,26] Experiments that look at the relative spatial arrangement of the amphiphilic templates with respect to the silica framework are thus quite scarce, since most of the solid state NMR characterisation concerns the porous samples after removal of the templating agents.[27]

In this work, we have chosen to investigate the solid state NMR responses of two silica-surfactant mesophases characterised by the same 2D-hexagonal (p6m) symmetry, prepared with the same templating agent, cetyltrimethylammonium bromide (CTAB), but one under acidic (HCl) conditions and one under basic (NaOH) conditions. They correspond to the so-called SBA-3[28] and MCM-41[29]-type silicas, respectively. Because of different synthesis pathways, the proposed interaction mechanisms are different.[30] In basic medium, a direct $S^{+}I^{-}$ interaction is proposed between the positively charged surfactant (S^{+}) and the negatively charged silica matrix (I^{-}). In acidic medium, interactions with surfactant micelles are mediated by a negatively charged counter-ion (X^{-}) whose presence is demonstrated by elemental analysis.[30] The interaction would be of type $S^{0}X^{-}I^{+}$, which accounts for a direct charge neutralisation between the counter-ion and the surfactant. Indeed the weak interaction that is assumed between the template and the silica framework in these samples is in agreement with the mild conditions required to remove the surfactant (reflux in ethanol) compared to the necessity to use acidic conditions when working with MCM-41 type systems.[30] Once again, this example illustrates the importance of a good understanding of the silica/surfactant interfaces in the as-prepared samples. Our

objective was thus to see whether NMR techniques could be sensitive to the different silica-surfactant interaction mechanisms, that have been proposed in the literature, and that assume longer distances between the surfactant polar head group and the silica surface when acidic conditions are used instead of basic conditions. Indeed, to our knowledge no detailed study has been published concerning interactions in the final material, between silica and cationic surfactants, like quaternary ammonium salts, though such templating agents have been widely used to prepare ordered mesoporous materials.

Preliminary 2D- $^{29}Si\{^{1}H\}$ HETCOR experiments have been recorded on both types of samples and different NMR responses were obtained.[31] Two contact times – time during which the magnetisation transfer occurs between the ^{1}H and ^{29}Si spin systems – were used to explore increasing inter-nuclei distances; these 2D-experiments are quite time-consuming especially with a moderate static magnetic field, which limits the number of possible contact times. Indeed, in most of the previous publications, only one experiment recorded at only one contact time has been presented. Considering the valuable information that can be extracted from these experiments with a variation of contact times, we have developed a new sequence based on a double CP transfer, a first transfer from ^{1}H to ^{29}Si, to select the Si sites close to protons, and essentially the surface sites, and then a second transfer back, from ^{29}Si to ^{1}H to detect only the signal of the protons which are dipolar coupled to these surface sites. Since it is a one-dimensional sequence, a complete variation of contact times can be recorded that allows exploring in a quasi-continuous way, the proximities between ^{1}H and ^{29}Si nuclei. Additional ^{1}H MAS-NMR experiments have been recorded with high spinning frequency on dehydrated and partially re-hydrated samples to look at the adsorbed water layers, while near infrared experiments, which are very sensitive the extent of hydrogen bonding involving water molecules, have completed the series of characterisations of the silica-surfactant interfaces of these two samples.

2. Experimental methods

2.1 Material synthesis

The CTAB/OH sample is prepared with the following conditions: 0.15 g of CTAB ($C_{16}H_{33}N^{+}(CH_3)_3Br^{-}$; Aldrich) are dissolved in a 3.85 wt% NaOH aqueous solution (8 g of NaOH in 200 ml of water). The solution was stirred until all surfactant was dissolved. 0.72 g of TEOS (Tetraethoxysilane; Fluka) are then added to the mixture under stirring. The final molar ratios are TEOS:CTAB:NaOH:H_2O = 1:0.12:0.5:120. The stirring of the solution (~ 500 rpm) was continued for 3 hrs, then filtered and dried during one day at ambient conditions and finally in the oven overnight at 100°C.

The synthesis of the CTAB/HCl sample follows the same steps. 0.10 g of CTAB are dissolved in an acidic aqueous solution composed of 0.12 g of water and 6.27 g of a 12.63 wt% (4 $mol \cdot L^{-1}$) HCl aqueous solution. The mixture is stirred for a few minutes before adding 0.5 g of TEOS. The final molar ratios are TEOS:CTAB:HCl:H_2O = 1:0.12:9.2:130. The filtering and the double drying processes are the same as in the CTAB/OH case.

2.2 Solid state NMR spectroscopy

^{29}Si MAS NMR spectra have been recorded on a Bruker AVANCE 400 (9.40 T) spectrometer. 7 mm zirconia rotors spinning at 5kHz have been employed. 324 transients have been collected with a 90° pulse of 6.5μs and recycle delays of 200s (CTAB/HCl) and 500s (CTAB/OH). These values have been chosen according to previous works found in the literature.[32,33] Spectra have been fitted with DMFIT2004 software.[34] ^{1}H MAS NMR spectra were recorded on a Bruker AVANCE 400 spectrometer with 2.5 mm zirconia rotor and with spinning frequency of 30 kHz. 8 transients have been collected with a 90° pulse of 3 μs and a recycling delay of 5 s. The chemical shift reference for the ^{1}H and ^{29}Si NMR experiments is tetramethylsilane (TMS; δ= 0 ppm).

Two-dimensional $^{29}Si\{^{1}H\}$ heteronuclear correlation (HETCOR) experiments and double Cross-Polarization $^{1}H \rightarrow ^{29}Si \rightarrow ^{1}H$ experiments have been recorded on a Bruker Avance 300 spectrometer with a CP-MAS probe and a 4 mm rotor spinning at 14 kHz. For the CP-HETCOR experiments, polarization transfer has been achieved by applying a constant radio-frequency (RF) field on the ^{29}Si channel

($\nu_{RF}(^{29}Si)$ = 50 kHz) while the RF field on the ^{1}H channel was ramped ($\nu_{RF}(^{1}H)$ = 50 ± 14 kHz). For the double CP experiments (sequence described in the text), cross-polarization transfers have been performed under adiabatic tangential ramps[35,36] in order to enhance the signal with respect to other known methods.[37] The pulse phasing was: $\phi_1 = (x_2, -x_2)$, $\phi_2 = (-x_2, x_2)$, $\phi_3 = (x, -x)$, $\phi_4 = (x_4, -x_4, y_4, -y_4)$, $\phi_5 = ((x, -x)_2, (y, -x)_2, (-y, x)_2, (-y, y)_2)$. For all experiments, two-pulse phase-modulated (TPPM) proton decoupling was applied during acquisition.[38] Quadrature detection in t_1 was realized using the STATES method.[39] Experimental conditions for the individual NMR experiments varied and are presented in detail in the figure captions accompanying the respective spectra.

2.3 Other analysis

X-ray diffraction patterns have been recorded with a Philips PW 1830 diffractometer equipped with a Cu-K_α source (λ = 1.54 Å), with a 0.02° step and an acquisition time of 5 s per point.

Elemental analysis was performed at the CNRS “Centre d’analyse élémentaire”, Vernaison (France).

Infrared absorption spectra were measured by a Fourier transform infrared (FTIR) spectrophotometer (Nicolet Nexus) mounted with a KBr-DTGS detector, in the 4000-400 cm^{-1} range; 256 scans with 4 cm^{-1} resolution. Near Infrared (NIR) spectra were measured in the 9000-4500 cm^{-1} range, using 256 scans with 4 cm^{-1} resolution. The spectra were recorded in absorption using anhydrous KBr powder, background was recorded using a KBr pellet prepared in the same condition. These experimental conditions assured that the effect of water absorption in KBr pellets from the external environment is not appearing in the infrared spectra. The beam splitter was CaF_2 and the detector was made of InGaAs.

3. Experimental results

3.1 – Characterization of the silica/surfactant bulk powders

The two samples CTAB/HCl and CTAB/NaOH have been characterized by X-ray diffraction, elemental analysis and ^{29}Si MAS NMR. The results are summarized in **Table 1**. Both samples have a 2-dimensional hexagonal structure (p6m) with very similar cell parameters (42.4 Å for CTAB/HCl and 41.4 Å for CTAB/NaOH). Elemental analysis reveals a higher surfactant/Si molar ratio in the final

powders (0.18 for CTAB/HCl and 0.21 for CTAB/OH) compared to the starting nominal composition (0.12). Under acidic conditions, an almost complete anionic exchange took place with the incorporation of 0.86 Cl^-, and only 0.05 Br^- in CTAB/HCl. The amount of anions ((Br+Cl)/N = 0.91) almost compensates the positive charge of the surfactant polar head group, which results in a fairly low expected charge on the silica network. This has already been noticed in the literature, as mentioned in the introduction.[30] On the contrary, the amount of residual anions in CTAB/OH is extremely low (Br/N = 0.08) in good agreement with a direct electrostatic interaction between the positively charged polar head group and the negatively charged silicate species.

The ^{29}Si MAS NMR spectra present peaks due to the three different silicon sites : Q_4= SiO_2, Q_3 = $SiO_{1,5}Ot$, Q_2 = $SiO(Ot)_2$ (Ot : Non-bridging oxygen).[31] The number of Q_3 sites is high in both samples, because of the rather short aging time of the powder after precipitation (3 h); ^{13}C MAS-NMR spectra (not shown) have confirmed the absence of any residual ethoxy groups. One might expect that under acidic conditions, the Q_3 units thus correspond to the presence of Si-OH groups, 0.64 per Si (including Q_3 and Q_2 contributions). Under basic conditions, a majority of $Si-O^-$ groups are expected but some Si-OH groups might also be present in the silica network. The percentage of each Si site (**Table 1**) shows that in basic medium (CTAB/OH) the network is slightly more condensed than in acidic medium (CTAB/HCl), a well-known result in sol-gel chemistry.[40]

The ^1H MAS NMR spectra of CTAB/HCl and CTAB/NaOH (see supporting information) show three main peaks at δ_{iso} = 0.9 ppm, 1.3 ppm and 3.3 ppm, respectively attributed to alkyl chain CH_3 protons, alkyl chain CH_2 protons (exception made for $N-CH_2$ in α-position) and polar head $N-CH_3$ and $N-CH_2$ protons.[41] Two additional peaks of lower intensity are detected around 4.5 ppm and 7.2 ppm for CTAB/HCl and 6.0 ppm for CTAB/OH. They certainly belong to surface silanols and/or surface water species. This will be discussed later on in the text.

3.2. Silica/Surfactant interfaces

3.2.1. ^{1}H-^{29}Si HETCOR experiments

Two-dimensional (2D) $^{29}Si\{^{1}H\}$ CP heteronuclear correlation (HETCOR) experiments have been recorded at two different contact times (t_{CP} = 500 μs and 5 ms) to probe the through-space proximities between ^{1}H and ^{29}Si sites (**Figure 1**). No specific thermal treatment was applied to the samples prior to these experiments.

CTAB/HCl sample

The experiment performed at t_{CP} = 500 μs is shown in **Figure 1**a. The 1D projection of the ^{29}Si MAS NMR signal along the F_2 dimension shows that almost only Q_3 sites are detected at short contact time. Interestingly, the main cross peak (A) represents a correlation between Q_3 silicon sites (δ = -100.9 ppm) and protons at 7.2 ppm that confirms its assignment to Si-OH protons. The other cross peak (B) corresponds to a correlation between Q_3 sites and N-CH_x (x=2,3) protons belonging to the surfactant polar head group (δ = 3.3 ppm). Its lower intensity, compared to (A) can be explained by a longer Si···H distance and by the higher mobility of polar head groups, two factors that contribute to decrease the efficiency of the polarization transfer between ^{1}H and ^{29}Si nuclei. The presence of a weak cross peak (C) between Q_4 sites (δ = -110.0 ppm) and N-CH_x protons is the signature of a longer distance between those species.

The experiment was repeated with t_{CP} = 5ms (**Figure 1**b). Here, the 1D projection of the ^{29}Si signal shows Q_3 as well as Q_4, and even Q_2 sites. New cross-peaks are now present. A weak one (E) is due to $Si(OH)_2$ species. Its absence in the previous experiment, despite short Si… H distances, is certainly related to a lack of sensitivity of the experiment to detect minor species. More interesting is the presence of the cross-peak (F) between Q_3 and protons in the alkyl chain at 1.3 ppm (presumably close to the polar head groups (β or γ positions)), together with the strong increase in intensity of the cross-peak (C). These observations demonstrate that a contact time of 5 ms allows exploring longer Si…H distances. Cross-peaks (A) and (B) are still observed, but with reverse intensity. Additionally, a cross peak appears between Q_3 and protons at 4.6 ppm, value that will be related later on to the presence of mobile water

molecules in weak interaction with Si-OH sites.

$^{29}Si\{^{1}H\}$ CP-HETCOR experiments were recorded with ^{1}H Lee-Goldburg homonuclear decoupling during contact time (CP-LG).[42] The use of ^{1}H pulses under Lee-Goldburg conditions (proton irradiation is shifted in frequency in order to average out the ^{1}H homonuclear dipolar interaction to first order[43]) eliminates most of the ^{1}H spin diffusion process that takes place during classical CP. The intensities of the cross peaks between Si-OH and Q_3 and Q_4 are slightly higher for the CP-LG HETCOR (see supporting information), which suggests that for a contact time of 5 ms, spin diffusion might occur between the protons of the Si-OH groups and the large reservoir of protons from the surfactant molecules. This will be confirmed later on in this work by 2D- $^{1}H\{^{1}H\}$ homonuclear correlation experiments.

CTAB/OH sample

The $^{29}Si\{^{1}H\}$ CP HETCOR experiment performed at t_{CP} = 500μs is shown in **Figure 1**c. The HETCOR spectrum only shows one cross peak (B) that represents the correlation between the Q_3 sites (δ= -99.1 ppm) and the N-CH_x protons of the polar head groups (δ= 3.3 ppm). In contrast to the previous sample, no cross-peak (A) between Q_3 sites and Si-OH protons of significant intensity is observed: this strongly suggests that Q_3 sites are primarily of Si-O^- type, rather than Si-OH one, in agreement with the pH conditions used during the synthesis.

For a contact time t_{CP} = 5ms (**Figure 1**d), the cross peak (B) is still of highest intensity, but two new cross-peaks between the Q_3 sites and protons are now observed. They are related to ^{1}H at δ= 5.7 ppm (A) and at δ= 1.3 ppm (F) respectively. The latter signal corresponds to protons belonging to the surfactant alkyl chain, CH_2 groups in β or γ positions with respect to the polar head group, and it was already observed for CTAB/HCl sample. More interesting is the cross peak (A) that can be assigned to water molecules hydrogen-bonded to Si-OH groups. Its non-observation at lower contact time is in agreement with high mobility, like protons in rapid exchange between surface Si-O^- or Si-OH groups. Similar results have already been shown in literature.[44] As for the Q_4 sites (δ= -109,3 ppm), one main

cross peak is observed (C) that represents correlation with the N-CH_x protons of the polar head groups. In contrast with CTAB/HCl sample, one cross peak (G) is also observed between Q_4 and CH_2 groups of the surfactant alkyl chain, suggesting a shorter Si…. H distance between the corresponding species in CTAB/OH compared to CTAB/HCl.

3.3.2. ^{1}H-^{29}Si-^{1}H double CP experiments

The 2D HETCOR spectra are very informative, but very time-consuming (1 to 3 days) to record especially with a moderate magnetic field (here 7.05 T). That is the reason why we have implemented a double cross-polarization sequence ^{1}H-^{29}Si-^{1}H (**Figure 2**) to record in a one-dimensional experiment the ^{1}H NMR spectrum, equivalent to the ^{1}H dimension of the HETCOR experiment, but with enhanced resolution. The acquisition of each 1D ^{1}H spectrum takes 1 hour. The sequence consists in a first polarization transfer from ^{1}H to ^{29}Si (characterized by a contact time t_{CP1}), followed by a second polarization transfer back to the nearby protons (with a second contact time t_{CP2}). The first contact time will be chosen in order to optimise the ^{29}Si signal intensity, while the second contact time will be incremented to reveal progressively the type of protons characterized with increasing internuclear distances from Si sites.

Such an approach is not new in literature since a number of pulse sequences exploiting double or multiple cross-polarization steps among two or three nuclei already exist. They are mainly used to select and enhance signals from specific nuclei in biochemical compounds[45] Despite the large number of published sequences, we have used a different approach that is more suitable for our studied system and the desired information. The main difference between our sequence and those found in literature concerns the way of eliminating residual proton magnetization after the first CP transfer and the consequent X nucleus protection (block B in **Figure 2**b). After the first CP transfer, magnetization of X nucleus is flipped back to the +z direction in order to minimize self-relaxation effects. Then, saturation of residual ^{1}H signals is achieved by a combination of a time-decreasing loop and $\pi/2$ pulses at the end

of each loop, which reveals to be very efficient even in case of different ^{1}H transversal relaxation times, $T_2(^1H)$. This saturation step has two goals: suppression of all unwanted ^{1}H signals and, within the model of thermal reservoirs[46], transformation of the proton bath into a hot reservoir into which magnetization can be back-transferred from the cold reservoir composed of X nuclei. After that, X magnetization is flipped back into the transversal plane before the second CP transfer. As we will see, the sequence reveals to be quite sensitive for our systems with results comparable and complementary to the previously used two-dimensional HETCOR techniques. The main drawback is the need for long relaxation times T_1 for X nucleus, but this is fully satisfied in our systems for which $30s \leq T_1(^{29}Si) \leq 100s$. **Figure 3** demonstrates the efficiency of the technique to detect the protons, close to the silica surface through the comparison of the ^{1}H MAS NMR spectra of CTAB/HCl acquired either via direct ^{1}H signal detection (**Figure 3**a) or through the ^{1}H-^{29}Si-^{1}H double CP sequence (**Figure 3**b). The protons at 7.2 ppm due to Si-OH are clearly visible with the new sequence as well as the $N(CH_x)$ protons due to the polar head groups, while those due the surfactant chains, which constitute indeed the major part of the proton bath are hardly detected.

Figure 4 shows a comparison between the ^{1}H-^{29}Si-^{1}H double CP experiments recorded on CTAB/HCl and CTAB/OH for a series of the second contact time t_{CP2}. These experiments were recorded after a thermal treatment of the samples overnight at 100°C to minimize the presence of adsorbed water. The value of t_{CP1} (3 ms) was chosen in order to optimize the polarization of the ^{29}Si nuclei after the first transfer, and it primarily concerns the Q_3 sites. The spectra for CTAB/HCl (**Figure 4**a) show a rather broad peak around 7 ppm due to Si-OH groups, for short t_{CP2} (100 μs). Its intensity increases with t_{CP2} reaching a maximum value for 5 ms, before a decrease in intensity due to $T_{1\rho}(^1H)$ relaxation effects. On the contrary, the spectra of CTAB/OH (**Figure 4**b) show no similar signal; one can only notice an undefined broad signal ranging from 5 to 15 ppm that may be related to some type of OH groups. This signal can be related to the peak observed at ≈ 10.5 ppm in high silica zeolites templated with trimethylalkylammonium compounds.[47] It was assigned to silanols hydrogen bonded to a siloxy goup,

SiO^-...HOSi, with an O....O distance of ≈ 2.7 Å. This weak signal in the CTAB/OH sample confirms the low content in Si-OH groups. One remarkable feature in the spectral evolution is the appearance of the signal at 3.3 ppm due the $N(CH_x)$ polar head protons. It is already detected at t_{CP2} = 100 μs for CTAB/OH, while for CTAB/HCl, it appears only for $t_{CP2} \geq 300$ μs. Then for both samples, the detection of a signal at 1.3 ppm related to the CH_2 groups of the surfactant chain occurs at much longer time (≥ 7 ms).

The ^1H-^{29}Si-^1H double CP sequence proves thus to be very efficient to discriminate the various ^1H families depending on their distance from the Si sites. The possibility to record in a reasonable time a series of spectra at increasing contact times leads to valuable information regarding the spatial distribution of the species at the silica/surfactant interface. However, the one-dimensional nature of the experiment prevents a neat identification of the Si sites involved in the polarization transfer. We have first investigated the possibility to extend this sequence to a two-dimensional ^1H-{^{29}Si} CP HETCOR correlation experiment by insertion of a time increment, t_1, after the block B. This new sequence is analogous to the ^{29}Si-{^1H} CP HETCOR experiment shown previously, except that the detection channel is now ^1H, and no longer ^{29}Si. Consequently, we could expect to gain in resolution on the ^1H dimension, and this could be of great interest since the resolution on the indirect F_1 dimension is always limited by the number of acquirable spectra. A comparison between the two sequences recorded with similar experimental parameters shows very similar results.[48]

The sequence has also been modified (**Figure 5**) by coupling the ^1H-^{29}Si-^1H double CP block with a ^1H magnetization exchange experiment. This allows to see how the ^1H magnetization that has been selected via the ^1H-^{29}Si-^1H double CP, can be exchanged during a mixing time τ_m within the proton spin systems. **Figure 6** compares experiments recorded for three different mixing times on CTAB/HCl. For τ_m = 140μs (**Figure 6**a), only diagonal peaks are present showing no magnetization exchange between the three ^1H spin systems : Si-OH groups, polar head groups and surfactant chains. For τ_m = 1 ms (**Figure 6**b), two cross-peaks appear : (A) shows a correlation between Si-OH and the NCH_x groups,

while (B) corresponds to a correlation between the NCH_x groups and the protons of the chain. For τ_m = 10 ms (**Figure 6**c), the diagonal peak due to Si-OH groups has disappeared, and now a new cross-peak (C) is present between these Si-OH groups and the protons of the chain. By increasing the mixing time, the magnetization is progressively transferred from the surface silanols to the interior of the micelle. The fact that the transfer is going one-way is a consequence of the filtering effect of the ^{1}H-^{29}Si-^{1}H double CP block, which polarized primarily the Si-OH and polar head protons, with almost nothing on the protons of the surfactant chain. The magnetization will thus be transferred along the following pathway : Si-OH → Polar head →Chain.

3.2 – Characterization of the surface species

3.2.1. ^{1}H MAS-NMR

In order to better identify the surface species, the samples have been dehydrated during 24 h under vacuum (~10^{-2} mbar) at 100°C. The rotors were filled in a dry glove, and then water was added to the rotor to follow the re-hydration process of the powders. These experiments have been performed with MAS spinning rate of 30 kHz to get better spectral resolution.

CTAB/HCl sample : besides the three peaks at δ_{iso} = 0.9 ppm, 1.3 ppm and 3.3 ppm, assigned to the surfactant molecules, and that have been already described, the spectrum of the dehydrated CTAB/HCl sample (**Figure 7**a) shows an additional broad signal of low intensity centered around 7.2 ppm. Similar chemical shift values have been reported for fairly acidic protons or silanols in strong H-bonding[24,49,50] in contrast to isolated silanols that are characterized by resonance peaks around 1-2 ppm.[51] Indeed, this value is in perfect agreement with the ^{1}H chemical shift value found in the $^{29}Si\{^{1}H\}$ HETCOR spectrum, for the cross-peak assigned to the Si-OH groups of Q_3 sites. When 1 mg of water is added to the powder, a new signal appears that can be decomposed into two peaks: a broad one at 4.8 ppm and a sharper one at 4.5 ppm. After a second addition of water (0.8 mg), the area of the 4.8 ppm peak does not change much while the area of the 4.5 ppm peak increases 3 times as much. The peak at 4.8 ppm can be

assigned to H_2O molecules in strong H-bonding with surface Si-OH groups.[27] The second one could be due to H_2O molecules as well, but in weaker interaction. Interestingly, with water addition, the signals due to the surfactant sharpen especially those due to the protons of the polar head. This is a result of an increasing mobility, and suggests that water molecules reached the interfacial silica/surfactant layer. The rotor was then placed under a IR lamp during 15 minutes for drying. The resulting ^1H spectrum is quite similar to the starting one obtained after dehydration, with even the re-appearance of the peak at 7.2 ppm that progressively broadened and shifted during water addition.

CTAB/OH sample : In contrast to the CTAB/HCl sample, the ^1H MAS NMR spectrum of dehydrated CTAB/OH (**Figure 7**b) hardly shows any detectable signal around 6-8 ppm, due to surface silanols in perfect consistency with the double CP results. After water addition (2.4 mg), two new signals can be identified, one rather broad at 5.3 ppm and one sharp at 4.6 ppm. Further water addition (1.4 mg) does not cause any important modification of the spectrum, besides the increase in intensity of the peak at 4.6 ppm, which is clearly due to highly mobile H_2O molecules, while the peak at 5.3 ppm can be assigned to H-bonded molecules. Further drying of the powder causes the total disappearance of the sharp peak, consistent with its assignment to free water molecules. But the signal around 5.3 ppm is still present and presents several components. In contrast to CTAB/HCl sample, a rather intense peak due to H-bonded H_2O is still present, which could suggest a certain difficulty for the water molecules to escape from the interfacial zone if we consider a strong interaction between water molecules and surface silanols.

3.3.2. FTIR and FT-NIR experiments

Figure 8a shows the FTIR absorption spectra, in the 4000-450 cm^{-1} range, of CTAB/HCl (dot line) and CTAB/OH (full line) samples. The spectra have been normalized with respect to the intensity of the 1050 cm^{-1} band. This main intense band is assigned to Si-O-Si antisymmetric stretching modes[52], and is accompanied with the symmetric stretching and rocking bands around 800 and 450 cm^{-1}, respectively, which represent the signature of the silica network. The 1050 cm^{-1} vibrational mode is accompanied by

another band around 1230 cm^{-1} that is assigned to the antisymmetric longitudinal optical mode (LO_3)[52]. A sharp intense band is present at 1160 cm^{-1}, this band is overlapped with the silica stretching band at 1050 cm^{-1} and can be clearly observed in the CTAB/HCl sample but not in CTAB/OH. The presence of this band can be correlated to the presence of cyclic or cage-like silica-based species or disordered induced modes[53]. Even if a specific attribution requires a detailed investigation that is beyond the purpose of this work we can, however, deduce that this mode is an indication of different structural features present in the silica backbone. The basic and acidic synthesis produced structural differences, as also indicated by the band at 580 cm^{-1}, which is due to four-fold silica rings[54], and is more intense in the CTAB/OH sample. The presence of the 1160 cm^{-1} band in CTAB/HCl certainly accounts for a different nature in the silica structure with respect to CTAB/OH.

Another informative band is observed at 1640 cm^{-1} ($\nu_b(H_2O)$), this band is assigned to molecular water and clearly shows that the water content in the CTAB/OH is higher than in CTAB/HCl. The bands between 2700 and 3000 cm^{-1} are due to the C-H stretching vibrations from the surfactant molecules and are related with the corresponding deformation bands between 1400 and 1500 cm^{-1}.[55] The region between 3000 and 3600 cm^{-1} corresponds to the O-H stretching vibrations from silanols and water species. The wide band is formed by several overlapped vibrational modes and, in general, a detailed attribution requires complex deconvolution methods. The spectra show, however, some distinctive features that can give some valuable information. The first one is related to the pore surface, the spectra suggest, in fact, the presence of longer H-bonded chains due to adsorbed water and surface silanols in the CTAB/HCl with respect to CTAB/OH. The maximum falls, in fact, around 3326 cm^{-1} for CTAB/HCl instead of 3468 cm^{-1} for CTAB/OH, furthermore the band appears sharper, which is a supporting indication of shorter silanol chains. The shoulder appearing at 3632 cm^{-1} mainly in CTAB/OH sample indicates the presence of terminal silanols with a weaker H-bonding character. Their presence can be associated to a higher degree of condensation in CTAB/OH. In both samples, we can note the absence of a peak due to isolated surface silanols around 3750 cm^{-1}.

In the OH stretching region the presence of molecular water can be followed using the first overtone of the bending mode of H-bonded water ($2\nu_b$), which falls around 3200 cm^{-1}. The broadness of the HCl band, which overlaps the $2\nu_b$, band of water, does not allow, however, a direct comparison between the two samples.

Bands in the NIR region (**Figure 8**b) account for the first overtones of ν(OH) stretching vibrations between 6800 and 7300 cm^{-1} and combinations of ν(OH) and δ(HOH) vibrations between 5000 and 5300 cm^{-1}. CH groups from CTAB resonate in the 5500-6000 cm^{-1} and 4000-4500 cm^{-1} regions and they will not be discussed here. The various types of water molecules interacting with the surface of silica have been discussed in a publication from Perry *et al.*[56] in terms of S'_0, S'_1, S'_2 species. S'_0 corresponds to a water molecule bonded to a silanol group through an oxygen atom; S'_1 to a water molecule bound to SiOH group *via* oxygen and hydrogen-bonded to one other water molecule; S'_2 to a water molecule bound to SiOH group *via* oxygen and hydrogen-bonded to two water molecules. Bands due to combinations of ν(OH) and δ(HOH) vibrations are expected at 5285 cm^{-1} and 5128 cm^{-1} for S'_0 and (S'_1,S'_2) respectively. A main difference is observed between CTAB/HCl and CTAB/NaOH samples, indicating that water molecules exhibit weaker interactions with the surface in CTAB/NaOH (dominant band due to S'_0) in agreement with data in the middle infrared. In CTAB/HCl material, water tends to strongly hydrogen-bond to surface silanols (bands at 5245 cm^{-1} and 5134 cm^{-1} assigned to S'_1 and S'_2). Presence of S'_2 water species should account for the formation of long range H-bonded chains and multilayers at silica surface.

4. Discussion

The combination of two-dimensional ^{29}Si-{^1H} HETCOR and one-dimensional ^1H-^{29}Si-^1H double CP spectra clearly show different responses for the CTAB/HCl and CTAB/OH. At short contact times (500 μs), only ^1H nearest neighbors to Q_3 sites are selected. In CTAB/HCl material, the related high chemical shift value (δ= 7.2 ppm) suggests the high acidic character of the protons as previously discussed. The

presence of some Si-OH_2^+ species along with Si-OH ones probably completes the picture of the silica surface. The only fact against a massive presence of Si-OH_2^+ species, though in perfect agreement with the synthesis conditions used for the CTAB/HCl material, is the almost 1:1 $(Cl^-+Br^-)/N^+$ molar ratio (**Table 1**), indicating that charge matching with the positive charge of the polar head group, CTA^+, is almost completely accomplished through the presence of the Cl^- counter-ions. Indeed, a correlation between Q_3 sites and the protons of the surfactant polar head exists, demonstrating the very close proximity between these two species despite the presence of the counter-ion. In the CTAB/OH sample, the absence of correlation between Q_3 sites and OH-type protons for 500 μs contact time, suggests that the majority of Q_3 sites is composed of Si-O^- species as previously discussed in perfect agreement with initial basic conditions. Consequently, Q_3 sites are in strong interaction with the protons of the CTA^+ polar head groups, as shown by the intense and lone correlation present in the corresponding HETCOR spectrum.

For longer contact times (5ms), the two systems still present different behaviors, especially for the OH surface species (Si-OH as well as H_2O). In both samples, Q_3 sites strongly interact with the CTA^+ polar head protons (N-CH_x) as well as with the CH_2 groups of the surfactant chain certainly in β or γ positions with respect to the polar head group. The main difference regarding the correlations involving the protons of the surfactant molecules is the intense cross peak between the CTA^+ polar head protons and Q_4 sites that is detected only in the CTAB/OH sample. It corresponds to a stronger ^{29}Si-^{1}H heteronuclear dipolar interaction between the $N^+(CH_3)_3$ protons and the Si surface sites, that could be attributed to shorter distances existing between the positively charged polar head of surfactant and the silica walls. However, one may keep in mind that these systems can not be considered as rigid ones. Indeed, the relatively good resolution of the ^{1}H MAS-NMR spectra recorded at relatively low spinning frequency (14 kHz; see supplementary information) is clearly due to internal mobility of the constitutive species that lead to a partial averaging of the strong ^{1}H homonuclear dipolar couplings. This prevents a direct correlation between the CP responses and the ^{29}Si-^{1}H internuclear distances.

Important structural information that can be extracted from the ^{29}Si-^{1}H CP-based NMR experiments is the apparent differences in the OH species present at the silica-surfactant interfaces. At longer contact times (5 ms), the Q_3 sites show correlation with OH-type protons, characterized by different chemical shift values depending on the sample. In CTAB/HCl, the peak at 7.2 ppm (already detected at short contact time) is assigned to primarily Si-OH groups and possibly some Si-OH_2^+ species. Additionally a signal is now detected at 4.6 ppm assigned to H_2O molecules in interaction with the surface. In CTAB/OH, a ^{1}H resonance signal at 5.7 ppm appears. As previously hypothesized, the associated OH groups could be part of water molecules in interaction with the Si-O^- surface sites, since double-CP experiments perfomed on the dried sample does not show any explicit silanol peak.

To get a better description about these OH surface species, one can compare the ^{1}H MAS NMR experiments performed on dehydrated and partially re-hydrated samples. The spectra of the de-hydrated samples totally confirm the results extracted from the ^{29}Si-^{1}H CP-MAS NMR experiments with no evidence for any OH in the CTAB/OH sample and a signal at 7.2 ppm for CTAB/HCl that can be safely assigned to Si-OH and/or $SiOH_2^+$ groups. Due to the de-hydrated nature of the sample, one could rule out extensive H-bonding with H_2O molecules. But the high chemical shift value could be explained by the presence of short hydrogen-bond distances between the H-atom of a Si-OH group and the O-atom of a neighboring Si-O-Si surface site.[57] When water is added to the samples, the ^{1}H NMR responses are completely different for both systems. In CTAB/OH, a broad (δ = 5.3 ppm) and a sharp (δ = 4.6 ppm) distinct ^{1}H resonance signals are detected. The sharp one is undoubtedly due to free H_2O molecules that do not interact with the surface, if one considers the small linewidth of the peak. The broader one can be related to the peak at 5.7 ppm observed in the HETCOR experiment, and assigned to H-bonded H_2O molecules, certainly in interaction with Si-O^- surface sites. Interestingly, after the second water addition, only the peak due to free water increases indicating that water is no longer interacting with the surface. One possible scenario is that in CTAB/NaOH sample, the interfacial space is limited to accommodate a large amount of water molecules, and this is in agreement with the strong electrostatic interaction

between the CTA^+ polar head groups and the negatively charge silica walls. In CTAB/HCl sample, no sharp signal due to free water is detected even after the second water addition, indicating that all water molecules are able to interact with the silica surface. Two overlapped broad resonance signals at 4.8 and 4.5 ppm are now present. As previously seen, only the intensity of the peak at 4.5 ppm increases with the amount of added water. This peak is certainly due to H_2O molecules in weak interaction with the surface. However, the linewidth, which is larger that in the case of CTAB/OH, suggests that the water molecules are in a confined environment, and possibly in the silica surfactant interfacial layer. After the water addition steps, the peak due to Si-OH present at 7.2 ppm in the de-hydrated sample seems to progressively shift to lower chemical shift values, and to broaden. This indicates possible exchange mechanisms between the Si-OH surface groups and the water molecules. Indeed, the reported chemical shift value of 4.8 ppm for the second signal, indicate rather weak interactions between the water molecules and the silica surface, but certainly through extensive H-bonding.

Infrared, and more specifically near-infrared experiments, have confirmed for the two samples, distinct structures for the adsorbed water layers present at the silica-surfactant interface: water molecules exhibit weaker interactions with the surface in CTAB/NaOH sample, while they tend to strongly hydrogen-bond to surface silanols in CTAB/HCl sample, and to form long range H-bonded chains and multilayers at silica surface. The presence of these water layers in CTAB/HCl accounts for the large decrease in line width of the ^1H resonance signal at 3.3 ppm due to the protons of the polar head groups, from 150 Hz in the de-hydrated sample down to 30 Hz after the second water addition. It indicates a higher mobility of the polar head groups, due to a higher solvation degree. This effect has already been discussed by Sizun *et al.*[58] who used methanol to increase the CTAB mobility. On the contrary, when water is added to the CTAB/OH sample, the peak linewidth does not vary with water addition, indicating that extensive solvation does not occur, due to strong electrostatic interactions between the polar head groups and the silica surface sites, which prevents the formation of water layers in the interfacial palisade.

All this study can allow proposing the schemes shown in for the surfactant-silica interfaces in CTA^+ templated samples prepared under acidic and basic conditions. The main difference comes from the existence of an extended network of H-bonded water molecules in the acidic case, which is certainly favored by the presence of hydrated Cl^- counter-ions.

5. Conclusion

This work has reinvestigated the structural study of CTAB-templated mesostructured silicas prepared under highly acidic and basic conditions. We have combined highly advanced 1D and 2D solid state NMR methods based on ^{29}Si-^{1}H dipolar coupling with Near Infrared spectroscopy in order to evidence the structural differences at the silica/surfactant interface that had been proposed through the so-called $S^+.I^-$ and $S^0.X^-.I^+$ interaction mechanisms. Indeed, we went one step further since we have clearly identified the presence of water molecules in the interfacial region that behave differently depending on the synthetic conditions. Silica obtained under acidic conditions shows a silanol-rich interface. Surfactant polar heads, whose charge is completely neutralized by its own counter-ion, settle close to the silanol palisade though leaving enough room to water molecules forming extended hydrogen bonding network. When silica is prepared under basic conditions, the surface is rich in SiO^- groups which are the lonely source for the neutralization of the polar head charge. This direct $SiO^-/N^+(CH_3)_3$ interaction induces a close proximity between surfactant polar head group and silica surface and it consequently prevents water molecules to largely interact with the silica surface.

Supporting Information Available. ^{1}H chemical shift values for CTAB/HCl and CTAB/OH samples. ^{1}H NMR-MAS spectra of CTAB/HCl and CTAB/OH samples. Comparison between the classical 2D ^{29}Si-{^{1}H} CP-HETCOR experiment and the 2D ^{1}H-{^{29}Si} CP-HETCOR experiment recorded with a pulse sequence based on the ^{1}H-^{29}Si-^{1}H double CP sequence. For CTAB/HCl sample, comparison between ^{1}H traces extracted from ^{29}Si-{^{1}H} CP HETCOR and CPLG HETCOR experiments for Q_3 (a) and Q_4 (b) sites. This material is available free of charge via the Internet at http://pubs.acs.org.

References

[1] a) Schuth, F. *Stud. Surf. Sci. Catal.* **2001**,135, 1.; b) Tanev, P.; Butruille, J.-R.; Pinnavaia, T. J. *Chemistry of Advanced Materials: An Overview*, Wiley-VCH, 1998.

[2] Soler-Illia, G. J. de A.A; Sanchez, C.; Lebeau, B.; Patarin, J. *Chem. Rev*., **2002**, *102*, 4093.

[3] Zhao, D.; Yang, P.; Huo, Q.; Chmelka, B. F.; Stucky, G.D. *Curr. Op. Sol. St. Mater. Sci.*, **1998**, *3*, 111-21.

[4] a) Lu, Y.; Fan, H.; Stump, A.; Ward, T.L.; Rieker, T.; Brinker, C.J. *Nature*, **1999**, *398*, 223 b) Baccile, N.; Grosso, D.; Sanchez, C. *J. Mater. Chem.*, **2003**, *13*, 3011.

[5] a) Brinker, C.J.; Lu, Y.; Sellinger, A.; Fan, H. *Adv. Mater.*, **1999**, *11*, 579; b) Grosso, D.; Babonneau, F.; Albouy, P.-A.; Amenitsch, H.; Balkenende, A.R.; Brunet-Bruneau, A.; Rivory, J. *Chem. Mater.*, **2002**, *14*, 931.

[6] Melosh, N. A.; Lipic, P.; Bates, F. S.; Wudl, F.; Stucky, G.D.; Fredrickson, G. H.; Chmelka, B.F.; *Macromolecules* **1999**, *32*, 4332-42.

[7] Sayari, A. *Chem. Mater*., **1996**, *8*, 1840.

[8] Corma, A. *Chem. Rev*., **1997**, *97*, 2373.

[9] Goettmann, F.; Grosso, D.; Mercier, F.; Mathey, F.; Sanchez, C. *Chem. Commun.*, **2004**, *10*, 1240-1241.

[10] Ciesla, U; Schuth, F. *Micro. Meso. Mater.*, **1999**, *27*, 131.

[11] a) Vallet-Regi, M.; Ramila, A.; del Real, R.P.; Perez-Pariente, J. *Chem. Mater.*, 2001, *13*, 308; b) Vallet-Regi, M.; *Chem. Eur. J.* (in press).

[12] Nicole, L.; Boissière, C.; Grosso, D.; Hesemann, P.; Moreau, J.; Sanchez, C. *Chem. Comm.*, **2004**, 2312.

[13] Balkenende, A.R.; de Theije, F.K.; Kriege, J.C.K. *Adv. Mater.*, **2003**, *15*, 139-143.

[14] Antochshuk, V.; Olkhovyk, O.; Jaroniec, M.; Park, I.-S.; Ryoo, R. *Langmuir*, **2003**, *19*, 3031-3034.

[15] Reddy, E.P.; Sun, B.; Smirniotis, P.G. *J. Phys. Chem. B*, **2004**. *108*, 17198-17205.

[16] Ying, J. Y.; Mehnert, C. P.; Wong, M. S. *Angew. Chem. Int. Ed.* **1999**, *38*, 56-77.

[17] Patarin, J.; Lebeau, B.; Zana, R.; *Curr. Op. Coll. Inter. Sci*., **2002**, *7*, 107.

[18] Brinker C. J.; Dunphy D. R.; *Curr. Op. Coll. Inter. Sci.* **2006**, *11*, 126-32.

[19] Galarneau, A.; Cambon, H.; Di Renzo, F.; Ryoo, R.; Choib, M.; Fajula, F. *New J. Chem.* **2003**, *27*, 73.

[20] Galarneau, A.; Cambon, H.; Di Renzo, F.; Fajula, F.; *Langmuir*,**2001**, *17*, 8328.

[21] Janicke, M. T.; Landry, C. C.; Christiansen, S. C.; Kumar, D.; Stucky, G.D.; Chmelka, B.F.; *J. Am. Chem. Soc.* **1998**, *120*, 6940-51.

[22] Janicke, M.T.; Landry, C.C.; Christiansen, S.C.; Birtalan, S.; Stucky, G.D.; Chmelka, B.F. *Chem. Mater.*, **1999**, *11*, 1342.

[23] Christiansen, S.C.; Zhao, D.; Janicke, M.T.; Landry, C.C.; Stucky, G.D.; Chmelka, B.F. *J. Am. Chem. Soc*., **2001**, *123*, 4519.

[24] Alam, T. M.; Fan, H.; *Macromol. Chem. Phys.* **2003**, *204*, 2023.

[25] Simonutti, R.; Comotti, A.; Bracco, S.; Sozzani, P.; *Chem. Mater.* **2001**, *13*, 771.

[26] Alonso, B.; Massiot, D.; *J. Magn. Res.* **2003**, *163*, 347.

[27] Trebosc, J.; Wiench, J.W.; Huh, S.; Lin, V.S.Y.; Pruski, M. *J. Am. Chem. Soc*., **2005**. *127*, 3057.

[28] Huo, Q.; Margolese, D.I.; Stucky, G.D. *Chem. Mater*., **1996**, *8*, 1147.

[29] Beck, J.S.; Vartuli, J.C.; Roth, W.J.; Leonowicz, M.E.; Kresge, C.T.; Schmitt, K.D.; Chu, C.T.W.; Olson, D.H.; Sheppard, E.W. *J. Am. Chem. Soc*., **1992**, *114*, 10834.

[30] Huo, Q.; Margolese, D.I.; Ciesla, U.; Feng, P.; Gier, T.E.; Sieger, P.; Leon, R.; Petroff, P.M.; Schüth, F.; Stucky, G.D. *Nature*, **1994**, *368*, 317.

[31] Baccile, N.; Maquet, J.; Babonneau, F.; *C. R. Chimie*, **2006**, *9*, 478.

[32] Steel, A.; Carr, S.W.; Anderson, M.W. *Chem. Mater*., **1995**, *7*, 1829.

[33] Goletto, V. Synthèse et Caractérisation d'Organosilices Mésostructurées à Porosité Périodique. PhD thesis, Université Pierre et Marie Curie-Paris6, Paris, **2002**; p 183.

[34] Massiot, D.; Fayon, F.; Capron, M.; King, I.; Le Calve, S.; Alonso, B.; Durand, J.-O.; Bujoli, B.; Gan Z.; Hoatson, G.; *Magn. Res. Chem.* **2002**, *40*, 70.

[35] Hediger S.; Meier, B.H.; Kurur, N.D.; Bodenhausen, G.; Ernst, R.R. *Chem. Phys. Lett.*, **1994**, *223*, 283.

[36] Hediger, S.; Meier, B.H.; Ernst, R.R., *Chem. Phys. Lett.*, **1995**, *240*, 449.

[37] Christiansen, S.C.; Hedin, N.; Epping, J.D.; Janicke, M.T.; del Amo, Y.; Demarest, M.; Brzezinski, M.; Chmelka, B.F. *Sol. St. Nucl. Magn. Res.*, **2006**, *29*, 170.

[38] Bennett, A.E.; Rienstra, C.M.; Auger, M.; Lakshmi, K.V.; Griffin, R.G. *J. Chem. Phys.* **1995**, *103*, 6951.

[39] States, D.J.; Haberkorn, R.A.; Ruben, D.J. *J. Magn. Reson.* **1982**, *48*, 286.

[40] Brinker, C. J.; Scherer, G.W. *Sol-gel Science : The physics and chemistry of sol-gel processing* Academic Press, Inc. **1989.**

[41] Alonso, B.; Harris, R.K.; Kenwright, A.M. *J. Coll. Inter. Sci*. **2002**, *251* 366.

[42] Van Rossum, B.-J.; Förster, H.; De Groot, H. J. M. *J. Magn. Res.* **1997**, *124*, 516-19.

[43] Lee, M.; Goldburg, W. I., *Phys. Rev.* **1965**, *140*, A1261.

[44] Gruenberg, B.; Emmler, T.; Gedat, E.; Shenderovich, I.; Findenegg, G.H.; Limbach, H.-H.; Buntkowsky, G. *Chem. Eur. J.*, **2004**, *10*, 5689.

[45] a) Seidel, K.; Etzkorn, M.; Sonnenberg, L.; Griesinger, C.; Sebald, A.; Baldus, M., *J. Phys. Chem. A*, **2005**, *109*, 2436; b) Mulder, F. M.; Heinen, W.; van Duin, M.; Lugtenburg, J.; de Groot, H. J. M., *J. Am. Chem. Soc.*, **1998**, *120*, 12891; c) Paulson, E. K.; Morcombe, C. R.; Gaponenko, V.; Dancheck, B.; Byrd, R. A.; Zilm, K. W., *J. Am. Chem. Soc.*, **2003**, *125*, 15831.

[46] Yannoni, C.S. *Acc. Chem. Res*, **1982**, *15*, 201.

[47] Koller, H.; Lobo, R.F.; Burkett, S.L.; Davis M.E. *J. Phys. Chem.* **1995**, *99*, 12588.

[48] See supporting information (Figure S2)

[49] Wolf, I.; Gies, H.; Fyfe, C.A. *J. Phys. Chem. B*, **1999**, *103*, 5933.

[50] Shenderovich, I.G.; Buntkowsky, G.; Schreiber, A.; Gedat, E.; Sharif, S.; Albrecht, J.; Golubev, N.S.; Findenegg, G.H.; Limbach, H.-H. *J. Phys. Chem. B*, **2003**, *107*, 11924.

[51] Bronnimann, C.E.; Zeigler, R.C.; Maciel, G.E. *J. Am. Chem. Soc.*, **1988**, *110*, 2023.

[52] Innocenzi, P. *J. Non Cryst. Solids*, **2003**, *316*, 309.

[53] a) *J. Phys. Chem. B* **2003,** *107*, 4711. b) Kirk, C. T. *Phys. Rev. B* **1988**, *38*, 1255.

[54] Yoshino, H.; Kamiya, K.; Nasu, H. *J. Non-Cryst. Solids* **1990**, *126*, 68.

[55] Ryczkowski, J.; Goworek, J.; Gac, W.; Pasieczna S.; Borowiecki, T. *Thermochimica Acta*, **2005**, *434*, 2.

[56] Perry, C.C.; Li, X. *J. Chem. Soc., Faraday Trans.*, **1991**, *87*, 761.

[57] Gervais, C.; private communication

[58] Sizun, C.; Raya, J.; Intasiri, A.; Boos, A.; Elbayed, K. *Micro. Meso. Mater.*, **2003**, *66*, 27.

Table 1. Structural parameters related to CTAB/HCl and CTAB/OH samples: cell parameter (a), chemical composition from elemental analysis data and distribution of Si sites from ^{29}Si MAS-NMR experiments. Error margins in ^{29}Si NMR analysis are estimated to ±1%.

Sample	a (Å)	N/Si (mol.%)	Cl/N (mol.%)	Br/N (mol.%)	Q_4		Q_3		Q_2	
					δ (ppm)	%	δ (ppm)	%	δ (ppm)	%
CTAB/HCl	42.4	0.18±0.01	0.86±0.03	0.05±0.01	-110.3	43	-100.9	50	-91.2	7
CTAB/OH	41.4	0.21±0.01		0.08±0.02	-109.2	48	-99.2	43	-90.5	9

Table 2. Assignments of the bands present in the FT-IR and NIR spectra of CTAB/HCl and CTAB/NaOH.

IR (cm^{-1})	Assignements	NIR (cm^{-1})	Assignements
580,1160	Cyclic species, Cubic octameric silica cages	4000-4500	C-H from CTAB
1050	AS-TO_3 Stretching	5130	$\nu_{OH} + \delta_{HOH}(S'_1, S'_2)$
1230	AS-LO_3 Stretching		
1630	Adsorbed water	5245	$\nu_{OH} + \delta_{HOH}(S'_0)$
2700-3000	C-H from CTAB	5500-6000	C-H from CTAB
3121	OH Stretching	6834	$2\nu_{OH}$ (S'_1, S'_2)
3234	H-Bonded water	7057	$2\nu_{OH}$ (S'_0)
3326	H-Bonded Si-OH chains	7177	$2\nu_{OH}$ (S'_0)
3468	H-Bonded Si-OH chains		
3632	Terminal silanols		

Table S1. ^{1}H chemical shift values for CTAB/HCl and CTAB/OH samples. The values for a solution of CTAB in D_2O ($5.10^{-2}M$) are given as references.

Chemical shift (ppm)			Assignment
CTAB/HCl sample	CTAB/OH sample	CTAB in D_2O	
0.9	0.9	0.85	CH_3 (C_{16})
		1.27	CH_2 (C_4-C_{15})
1.3	1.3	1.35	CH_2 (C_3)
		1.75	CH_2 (C_2)
3.3	3.3	3.17	N-CH_3
		3.42	N-CH_2 (C_1)
4.2-4.5	4.6		H_2O
4.4-4.8	5.3		Si-OH in interaction with H_2O
7.2			Si-OH in interaction with the surface

Captions for Figures A updater quand on aura modifié les légendes

Figure 1. Two dimensional HETCOR $^{29}Si\{^{1}H\}$ spectra recorded on CTAB/HCl with τ_{CP} = 500 μs (a) and τ_{CP} = 5 ms (b) and on CTAB/NaOH with τ_{CP} = 500 μs (c) and τ_{CP} = 5 ms (d). Experimental parameters (Number of transients : NS and number of acquired spestra in the reconstructed F_1 dimension : TD1) are the followings : a) NS= 800, TD1= 94 ; b) NS= 904, TD1= 32; c) NS= 2144, TD1= 32; d) NS= 904, TD1= 64. Contour levels base has been chosen from maximum and up to noise level.

Figure 2. Schematic principle of ^{1}H-^{29}Si-^{1}H double CP experiment and related NMR sequence.

Figure 3. Comparison between the ^{1}H MAS-NMR spectra of CTAB/HCl recorded with direct detection (a) and via the ^{1}H-^{29}Si-^{1}H double CP sequence (b).

Figure 4. ^{1}H-^{29}Si-^{1}H double CP NMR spectra recorded on CTAB/HCl and CTAB/OH for a series of the second contact time t_{CP2}.

Figure 5. Pulse sequence for the 2D ^{1}H homonuclear correlation spectra shown in Figure 7: ^{1}H-X-^{1}H double CP experiment combined with a ^{1}H magnetization exchange experiment characterized by the mixing time τ_m.

Figure 6. Two-dimensional homonuclear ^{1}H correlation spectra of CTAB/HCl taken using the pulse sequence shown in Figure 6, with various mixing times: (a) τ_m = 140 μs, (b) τ_m = 1 ms, (b) τ_m = 10 ms.

Figure 7. ^{1}H NMR-MAS spectra of CTAB/HCl (a) and CTAB/NaOH (b). (B_0 : 9.4 T – Sample spinning : 30 kHz)

Figure 8. Infra-red (a) and near Infra-red (b) spectra recorded on CTAB/HCl and CTAB/NaOH.

Figure 9. Schematic view of the silica-surfactant interfaces in CTAB/HCl and CTAB/NaOH samples

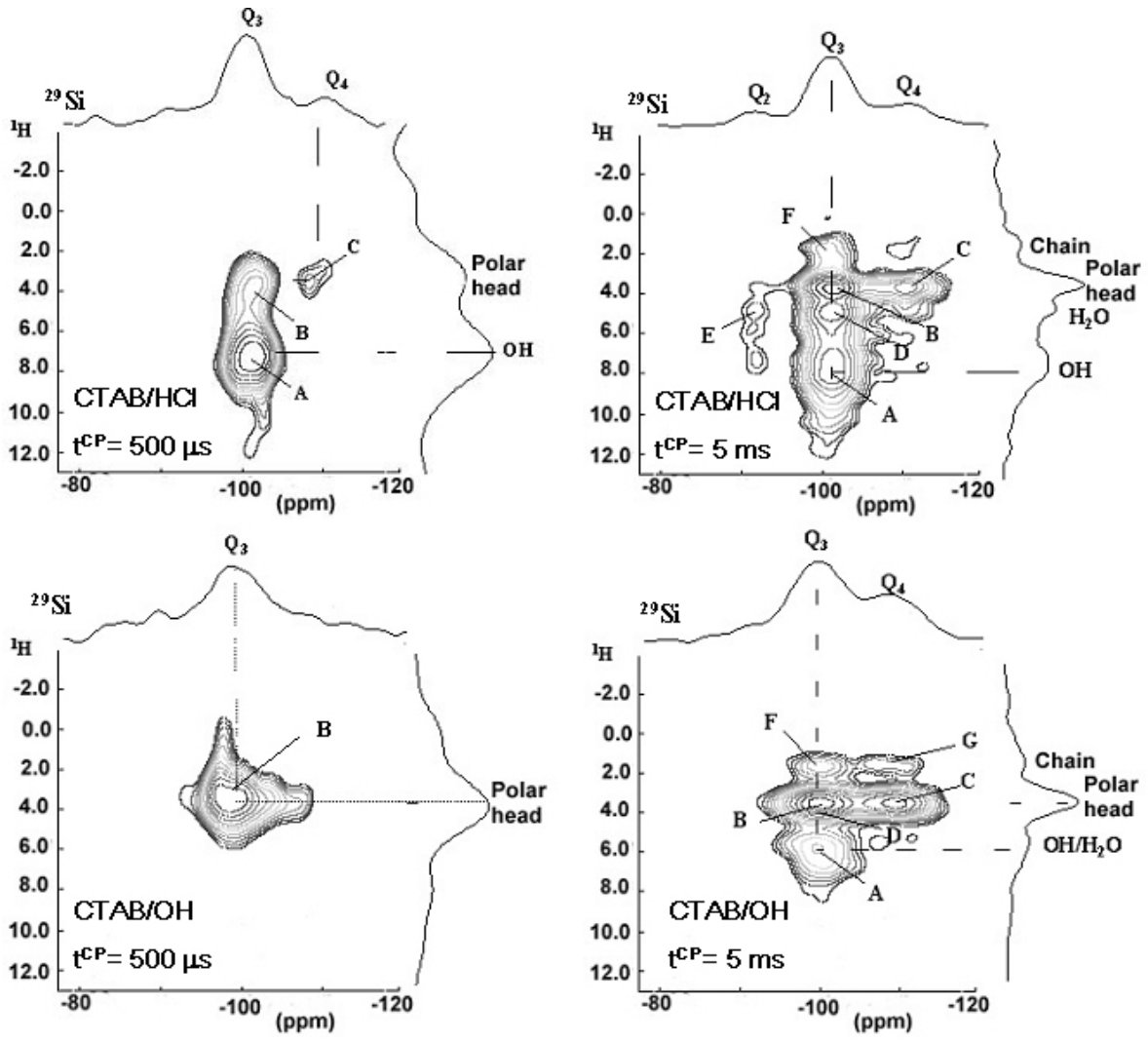

Figure 1. Two dimensional HETCOR $^{29}Si\{^{1}H\}$ spectra recorded on CTAB/HCl with τ_{CP} = 500 µs (a) and τ_{CP} = 5 ms (b) and on CTAB/NaOH with τ_{CP} = 500 µs (c) and τ_{CP} = 5 ms (d). Experimental parameters (Number of transients : NS and number of slices in second dimension : TD1) are the followings : a) NS= 800, TD1= 94 ; b) NS= 904, TD1= 32; c) NS= 2144, TD1= 32; d) NS= 904, TD1= 64. Contour levels base has been chosen from maximum and up to noise level. t_1 increments?

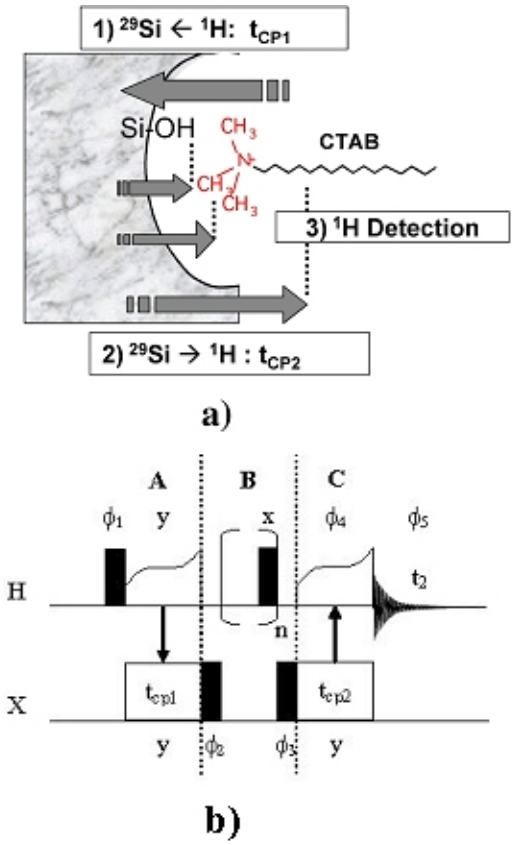

Figure 2. Schematic principle of ^{1}H-^{29}Si-^{1}H double CP experiment and related NMR sequence.

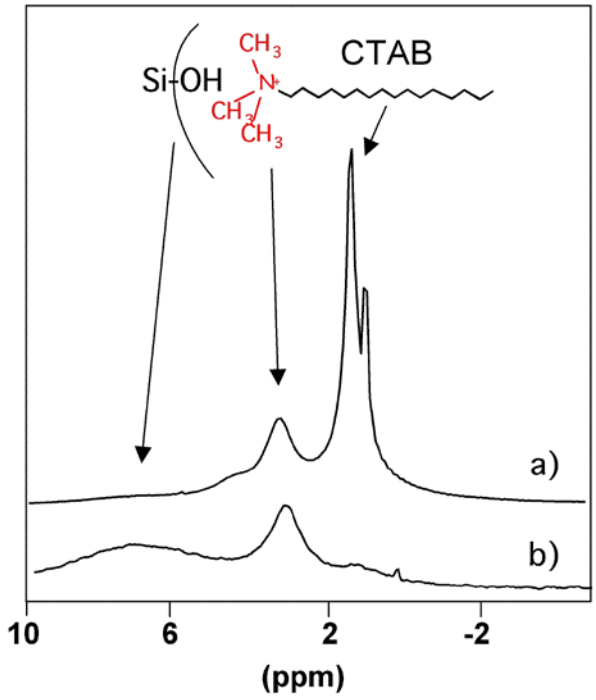

Figure 3. Comparison between the ^{1}H MAS-NMR spectra of CTAB/HCl recorded with direct detection (a) and via the ^{1}H-^{29}Si-^{1}H double CP sequence (b) with t_{CP1} = 3 ms and t_{CP2} = 5 ms.

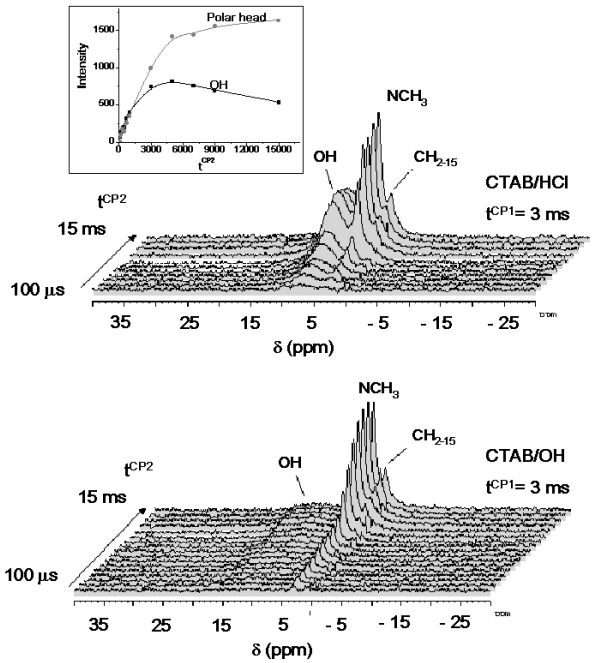

Figure 4. ^{1}H-^{29}Si-^{1}H double CP NMR spectra recorded on CTAB/HCl and CTAB/OH for a series of the second contact time t_{CP2} from 100 µs and 15 ms. Insert à enlever.

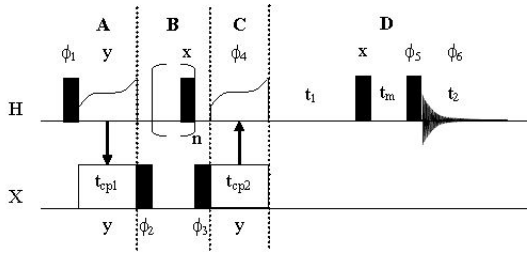

Figure 5. Pulse sequence for the 2D ^{1}H homonuclear correlation spectra shown in **Figure 6** : ^{1}H-X-^{1}H double CP experiment combined with a ^{1}H magnetization exchange experiment characterized by the mixing time τ_m.

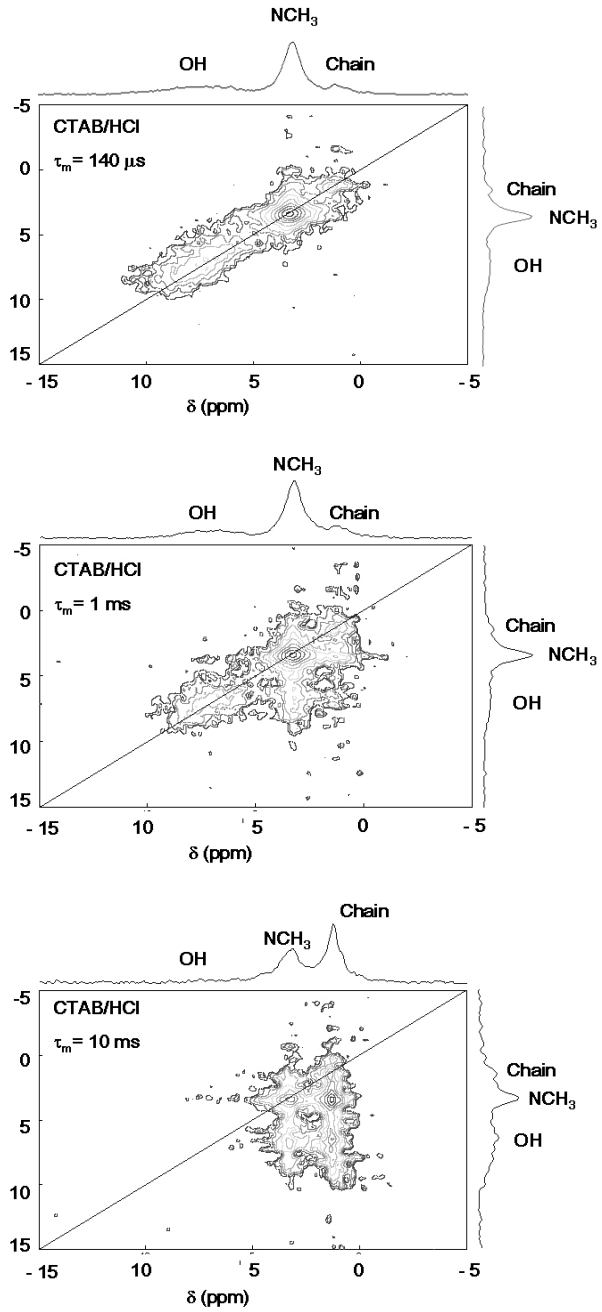

Figure 6. Two-dimensional homonuclear ^{1}H correlation spectra of CTAB/HCl taken using the pulse sequence shown in **Figure 5**, with various mixing times: (a) τ_m = 140 μs, (b) τ_m = 1 ms, (b) τ_m = 10 ms.

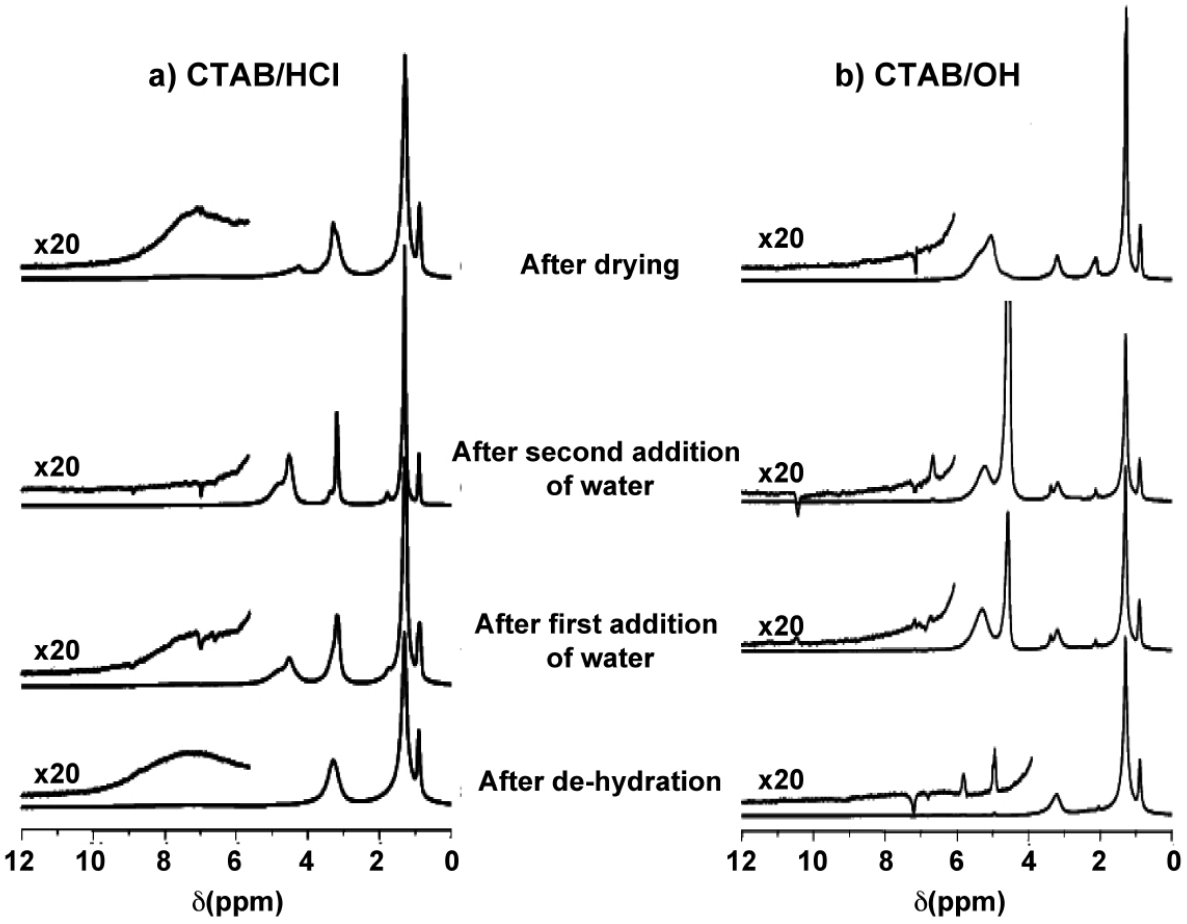

Figure 7. ^{1}H NMR-MAS spectra of CTAB/HCl (a) and CTAB/NaOH (b). (B_0 : 9.4 T – Sample spinning : 30 kHz)

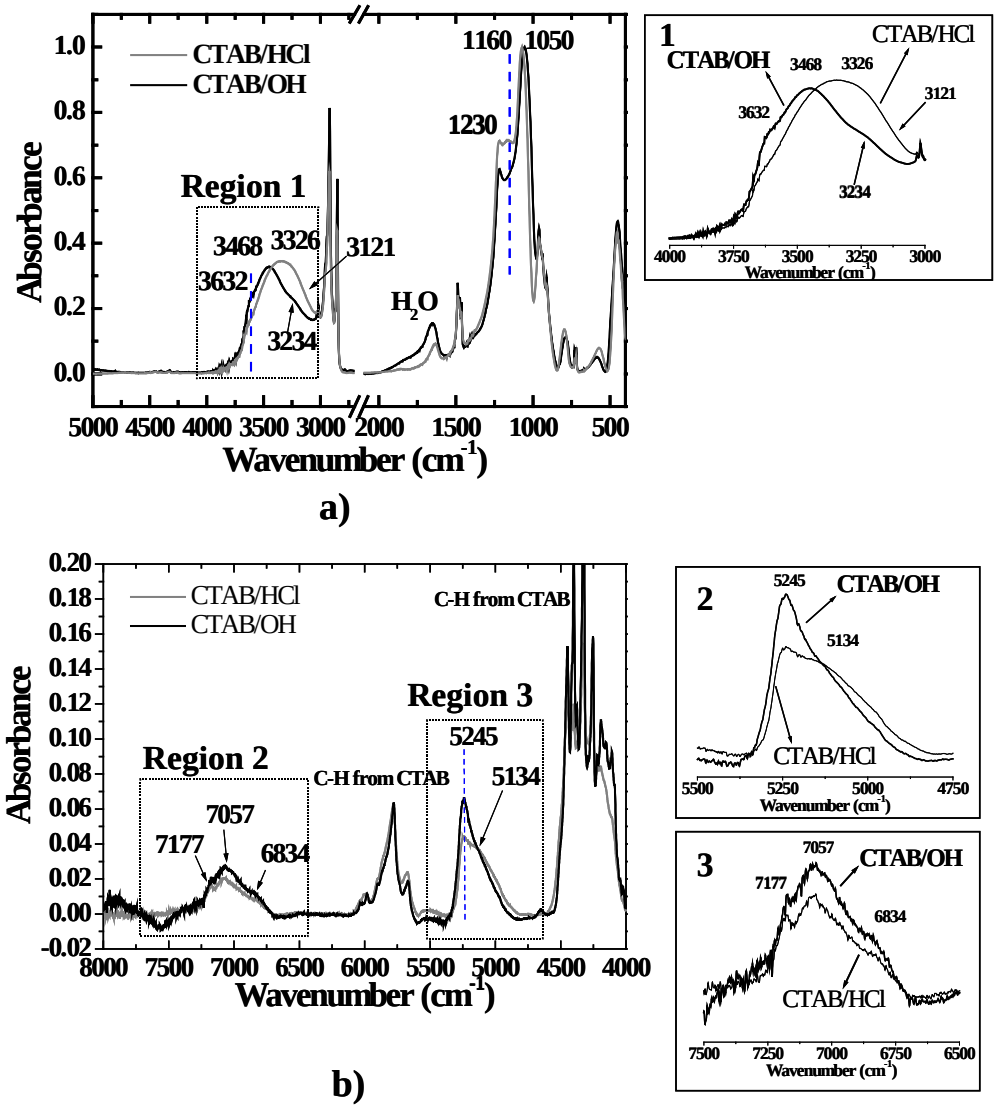

Figure 8. Infra-red (a) and near Infra-red (b) spectra recorded on CTAB/HCl and CTAB/NaOH. Ajouter legende

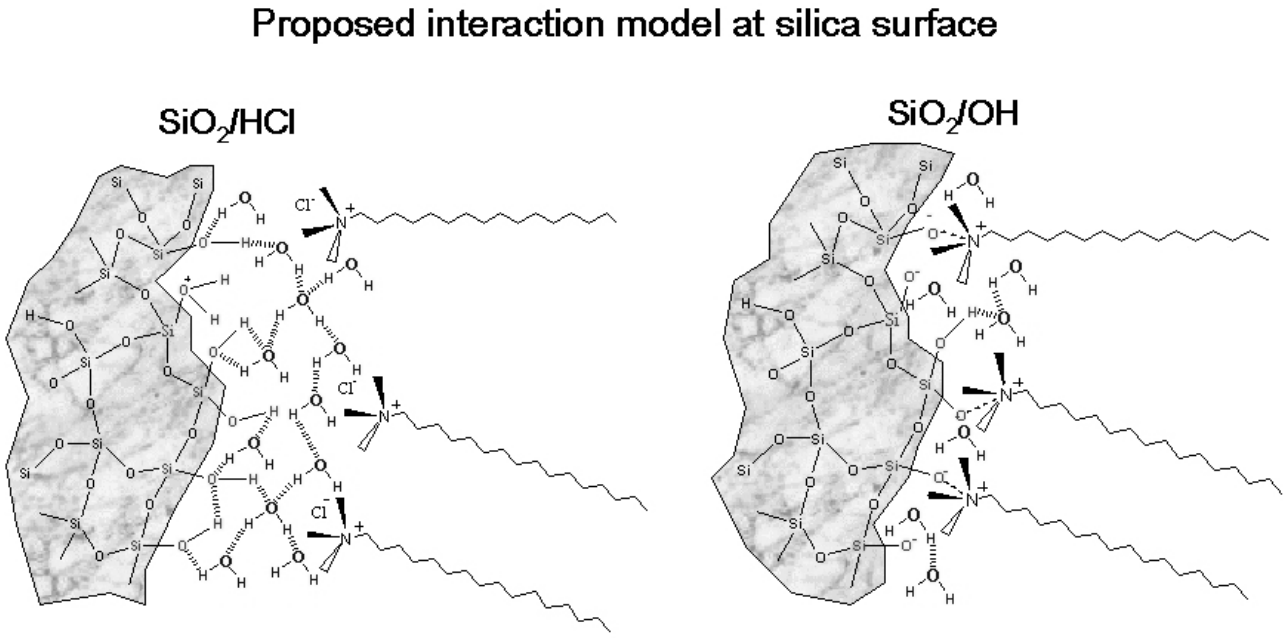

Figure 9. Schematic view of the silica-surfactant interfaces in CTAB/HCl and CTAB/NaOH samples

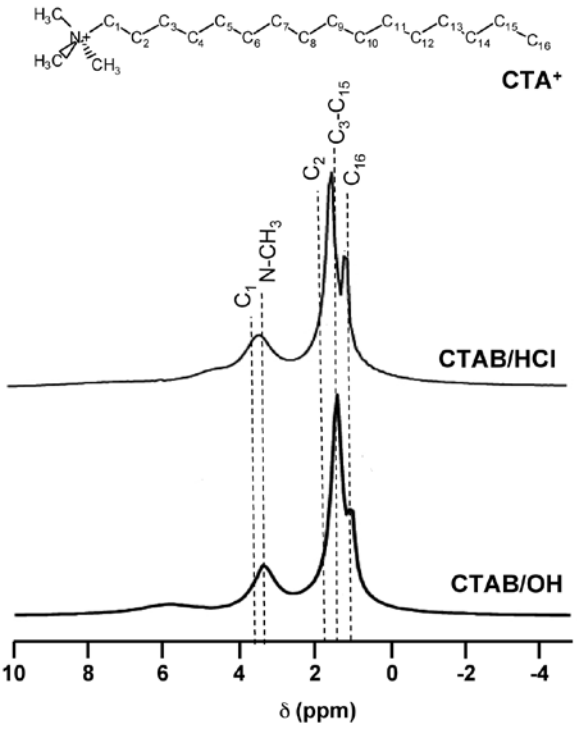

Figure S1. ^{1}H NMR-MAS spectra of CTAB/HCl and CTAB/OH samples. The dotted lines correspond to chemical shift values extracted from the ^{1}H NMR spectrum of a solution of CTAB in D_2O (5.10^{-2} M).

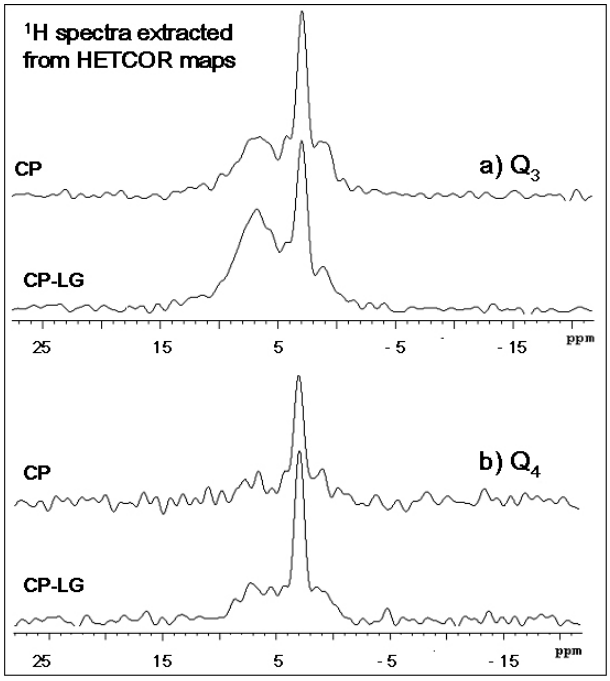

Figure S2. CTAB/HCl sample : comparison between ^{1}H traces extracted from $^{29}Si\{^{1}H\}$ CP HETCOR and CPLG HETCOR experiments for Q_3 (a) and Q_4 (b) sites.

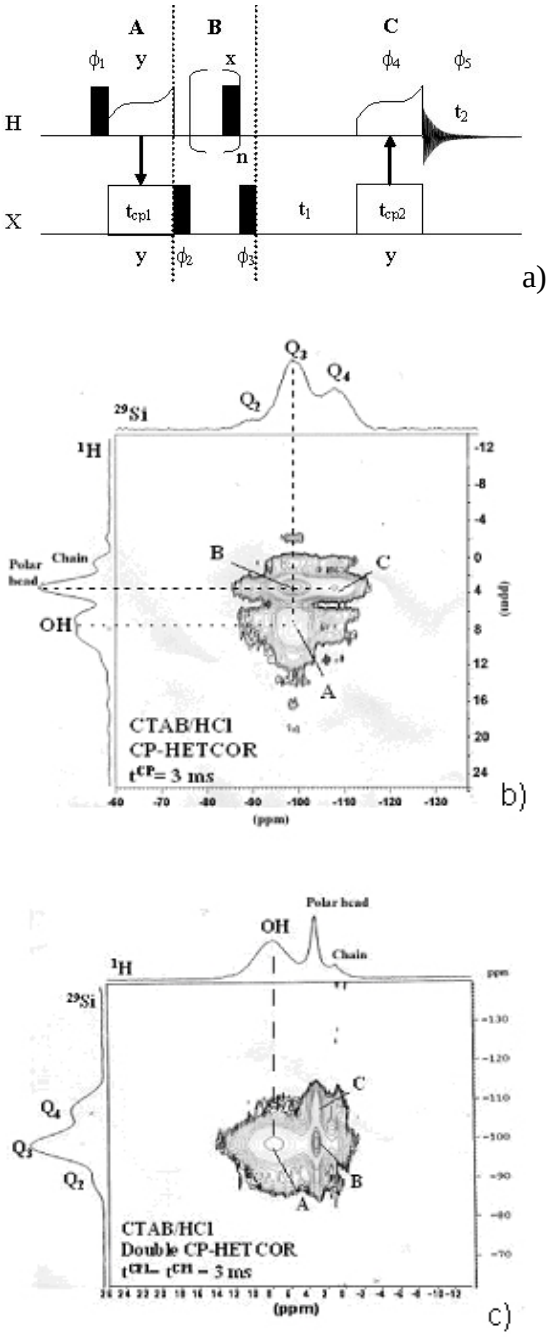

Figure S3. Comparison between the classical 2D ^{29}Si-{^{1}H } CP HETCOR experiment (b) and the 2D ^{1}H-{^{29}Si} CP HETCOR experiment (c) recorded with the pulse sequence based on the ^{1}H-^{29}Si-^{1}H double CP sequence (a).